

---

## IEEE Copyright Notice

© 2019 IEEE. Personal use of this material is permitted. Permission from IEEE must be obtained for all other uses, in any current or future media, including reprinting/republishing this material for advertising or promotional purposes, creating new collective works, for resale or redistribution to servers or lists, or reuse of any copyrighted component of this work in other works.

Accepted to be Published in:

Proceedings of the **2019 IEEE International Symposium on Hardware Oriented Security and Trust (HOST)**  
May 4-7, 2020, San Jose, CA, USA

This version of the paper is the one which was accepted during the review process.

The DOI will be added after publication.

---

# Statistical Ineffective Fault Analysis of GIMLI

Michael Gruber, Matthias Probst, Michael Tempelmeier

*Chair of Security in Information Technology*

*Technical University of Munich*

Munich, Germany

{m.gruber, matthias.probst, michael.tempelmeier}@tum.de

**Abstract**—Statistical Ineffective Fault Analysis (SIFA) was introduced as a new approach to attack block ciphers at CHES 2018. Since then, they have been proven to be a powerful class of attacks, with an easy to achieve fault model. One of the main benefits of SIFA is to overcome detection-based and infection-based countermeasures. In this paper we explain how the principles of SIFA can be applied to GIMLI, an authenticated encryption cipher participating the NIST-LWC competition. We identified two possible rounds during the initialization phase of GIMLI to mount our attack. If we attack the first location we are able to recover 3 bits of the key uniquely and the parity of 8 key-bits organized in 3 sums using 180 ineffective faults per biased single intermediate bit. If we attack the second location we are able to recover 15 bits of the key uniquely and the parity of 22 key-bits organized in 7 sums using 340 ineffective faults per biased intermediate bit. Furthermore, we investigated the influence of the fault model on the rate of ineffective faults in GIMLI. Finally, we verify the efficiency of our attacks by means of simulation.

**Index Terms**—Fault Attack, Statistical Ineffective Fault Analysis, SIFA, GIMLI, Authenticated Encryption, NIST

## I. INTRODUCTION

Fault attacks span a class of implementation level attack which were first introduced by Boneh et al. in their seminal work [2]. Fault attacks pose a serious threat to the implementation of cryptographic algorithms. They usually aim for a modification of the processed data or the control flow in order to reduce the underlying mathematical problem to a simpler one. The most common type of fault attack is the Differential Fault Analysis (DFA) which requires knowledge of multiple faulted encryptions and a correct one. Statistical Ineffective Fault Analysis (SIFA), as introduced by Dobraunig et al. [6], requires only an intermediate state with a biased distribution i.e. a distribution which deviates from the uniform distribution. Also, in contrast to Differential Fault Analysis (DFA) it is not necessary to have tuples of faulty and correct encryptions. Even worse, SIFA can break traditional countermeasures against fault attacks like detection-based or infection-based countermeasures.

**State of the art:** So far the principles of SIFA were applied to a variety of cryptographic algorithms ranging from block ciphers as AES [6] to authenticated encryption schemes like KETJE, KEYAK [5] and ASCON [11].

**Contributions:** We present the first SIFA on the NIST-LWC-candidate GIMLI. Additionally, we verify the efficiency of our

attacks by means of simulation. In addition, we evaluate the influence of the fault model on the rate of ineffective faults.

**Organization:** The rest of the work is structured as follows: Section II introduces authenticated encryption and the NIST-LWC competition. Section III explains the principles of SIFA. Section IV presents the NIST-LWC candidate GIMLI. Section V introduces our SIFA on GIMLI. Section VI provides the results of our proposed attack on GIMLI.

## II. NIST LIGHTWEIGHT CRYPTOGRAPHY

With the growing amount of interconnected devices, the need for secure communications is ubiquitous. While today's cryptographic algorithms are well suited for high-end computing, like servers, or desktops, their performance degenerates dramatically, when implemented on small, resource-constrained devices. Therefore, the National Institute of Standards and Technology (NIST) launched an open standardization project for lightweight cryptography in 2013 [8]. In 2019, the tremendous amount of 57 round 1 submissions confirms the need and interest of lightweight cryptography. NIST focuses on small, but secure algorithms that provide both Authenticated Encryption with Associated Data (AEAD) and Hash. Additional features like post-quantum resistance or ease of side-channel and fault-attack resistant implementations are desirable, but not mandatory. In this paper, we will focus on AEAD: Authenticated Encryption (AE) combines the traditionally separated cryptographic primitives *symmetric key cryptography* and *authentication* into one single algorithm. Additionally, in AEAD, Associated Data (AD) is authenticated, but not encrypted. This is particularly useful for header information in a communication protocol that must be authenticated, but do not need to be encrypted. If the authentication of either the AD or message fails, an empty string is output, otherwise the plaintext is released. This prevents chosen ciphertext attacks. Fig. 1 shows the inputs and outputs of an AEAD scheme (encryption). Formally, let  $k, \nu, t \geq 1$ ,  $K \in \{0, 1\}^k$  denote a secret key,  $N \in \{0, 1\}^\nu$  a nonce,  $AD \in \{0, 1\}^*$  associated data,  $M \in \{0, 1\}^*$  a message,  $T \in \{0, 1\}^t$  an authentication tag, and  $C \in \{0, 1\}^*$  a ciphertext. An AEAD is a triple  $\Pi = (\mathcal{K}, \mathcal{E}, \mathcal{D})$ , with a key-generation procedure  $\mathcal{K}$  that returns a random  $K$ , an encryption algorithm  $\mathcal{E}_K(N, AD, M)$ , and a decryption algorithm  $\mathcal{D}_K(N, AD, C, T)$ , where  $\mathcal{E}$  outputs a pair  $(C, T)$ , and  $\mathcal{D}$  outputs either the plaintext  $M$  or the void symbol  $\perp$  if the tag is invalid:

$$\mathcal{E} : \{0, 1\}^k \times \{0, 1\}^\nu \times \{0, 1\}^* \times \{0, 1\}^* \rightarrow \{0, 1\}^* \times \{0, 1\}^t$$

$$\mathcal{D} : \{0, 1\}^k \times \{0, 1\}^\nu \times \{0, 1\}^* \times \{0, 1\}^* \times \{0, 1\}^t \rightarrow \{0, 1\}^* \cup \{\perp\}$$

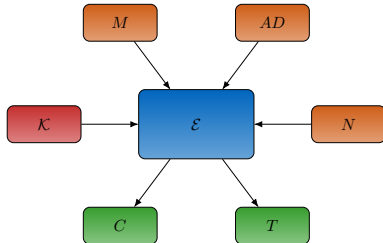


Figure 1: AEAD Encryption

### III. SIFA

The exploitation of statistical ineffective faults was first proposed by Dobraunig et al., in order to break symmetric cryptography [6]. SIFA can be seen as the combination of Ineffective Fault Analysis (IFA), as proposed by Clavier and Christophe [3], and Statistical Fault Analysis (SFA) as proposed by Fuhr et al. [7]. In the following, the principles of SIFA are explained.

#### A. Background

SIFA combines the benefits of IFA and SFA in terms of the required fault model, the key distinguisher and the ability of overcoming countermeasures: The required fault model of IFA, is rather specific e.g. Clavier et al. proposed a fault model where the computation of an XOR results always in a zero value [3]. The downside of the assumed fault model is the fact that the required fault model is difficult to achieve in practice. In contrast, the assumptions of the required fault model for a SFA are loose as the only requirement for a successful SFA is a biased intermediate state as shown by Fuhr et al. [7]. Both attacks differ significantly in how they recover the key: In IFA the recovery of the correct target partial sub key is strictly analytical; whereas in SFA a statistical approach is used. One of the main benefits of the statistical approach, in SFA, is the immunity to noisy faults i.e. injections that do not comply with the required fault model. The main benefit of ineffective faults is the ability to break common countermeasures against fault attacks. There are two possible countermeasures against fault attacks: detection-based countermeasures and infection-based countermeasures [6]. The most common form of detection-based countermeasures is temporal redundancy, where an encryption or decryption is performed twice. If the results do not match, a fault occurred and appropriate measures like a system-reset can be taken. The infection-based countermeasure applies additional operations in order to increase the fault propagation to a level where an attack is no longer feasible [9, 13]. IFA is based on a very precise fault model where a faulted operation always returns the same value in the general case. By forcing the output of an operation to a specific value, the attacker can distinguish, if the output of the faulty operation is equal to the fault free output. If the faulted output equals the fault free output, an ineffective fault occurred. Fig. 2-IFA shows this behavior, where the computation of an XOR always returns

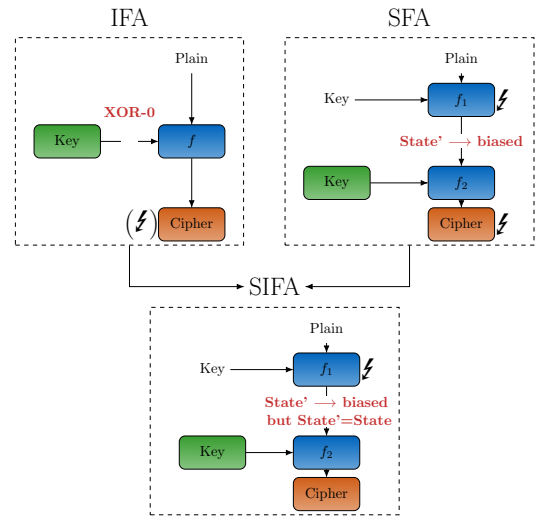


Figure 2: SIFA Background

zero as in [3]. IFA is feasible even if the previously introduced countermeasures are implemented because the output of the cryptographic operation is correct. In contrast to IFA, SFA exploits the non-uniform distribution of intermediate values in conjunction with the corresponding faulty output to recover the secret key. As shown in Fig. 2-SFA an attacker injects a fault after the computation of  $f_1$  and before  $f_2$ , where  $f_i \mid i \in \{1, 2\}$  denotes parts of the cryptographic operation. The intermediate state becomes therefore faulty and follows a biased distribution which enables a SFA. The attack partially decrypts the faulty ciphertext with a hypothesis of the target partial subkey in order to calculate the faulty (biased) intermediate value. By repeating this for all key-hypotheses and ranking the corresponding intermediate values according to their deviation from the uniform distribution. When SIFA is applied, an attacker can determine the correct key by introducing ineffective faults. However, in contrast to IFA the fault model does not need to be known exactly. It is sufficient to bias an intermediate value. Furthermore, the cipher-output needed for the attack is correct in contrast to SFA.

#### B. Foundations of Statistical Ineffective Fault Analysis

SIFA evaluates the statistical distribution of intermediate values and identifies appropriate key candidates with a statistical model.

**Distribution of Intermediate values:** We assume that a fault only corrupts a part  $s$  of the intermediate state. The partial intermediate state after a fault injection is denoted by  $s'$ . The alternation of  $s \rightarrow s' \mid s \neq s'$  results in a faulty computation and will affect the outcome of the cryptographic algorithm. However, an alternation  $s \rightarrow s' \mid s' = s$  does not affect the outcome of the cryptographic algorithm. From now on we will refer to such a behavior as an ineffective fault.

Such ineffective faults can be exploited, if they cause a biased distribution in the intermediate value. The six Fault

Distribution Tables (FDTs) in Table 1 show the transition probability of two-bit intermediate values for six typical fault models. In order to apply SIFA, the diagonal of such a table (marked in blue) must differ from the uniform distribution. This holds true for Tables 1a to 1d. The table's entries which are not colored blue denote the probability of effective faults.

		(a) Random-Or				(b) Random-And					
		s'				s'					
s	00	00	$\frac{1}{4}$	$\frac{1}{4}$	$\frac{1}{4}$	00	$\frac{1}{4}$	0	0	0	
	01	0	$\frac{1}{2}$	0	$\frac{1}{2}$	s	01	$\frac{1}{2}$	$\frac{1}{2}$	0	0
	10	0	0	$\frac{1}{2}$	$\frac{1}{2}$		10	$\frac{1}{2}$	0	$\frac{1}{2}$	0
	11	0	0	0	$\frac{1}{4}$		11	$\frac{1}{4}$	$\frac{1}{4}$	$\frac{1}{4}$	$\frac{1}{4}$
		s'					s'				
(c) Stuck-at-0		s'				s'					
		00	00	01	10	11	00	00	01	10	11
		00	$\frac{1}{4}$	0	0	0	00	$\frac{4}{9}$	$\frac{2}{9}$	$\frac{2}{9}$	$\frac{1}{9}$
		01	1	$\frac{1}{2}$	0	0	01	$\frac{4}{9}$	$\frac{2}{9}$	$\frac{2}{9}$	$\frac{1}{9}$
		10	1	0	$\frac{1}{2}$	0	10	$\frac{4}{9}$	$\frac{2}{9}$	$\frac{2}{9}$	$\frac{1}{9}$
(e) Random fault		s'				s'					
		00	00	01	10	11	00	00	01	10	11
		00	$\frac{1}{4}$	$\frac{1}{4}$	$\frac{1}{4}$	$\frac{1}{4}$	00	$\frac{1}{4}$	0	0	1
		01	$\frac{1}{4}$	$\frac{1}{4}$	$\frac{1}{4}$	$\frac{1}{4}$	01	0	$\frac{1}{4}$	1	0
		10	$\frac{1}{4}$	$\frac{1}{4}$	$\frac{1}{4}$	$\frac{1}{4}$	10	0	1	$\frac{1}{4}$	0
(f) Bit-flip		s'				s'					
		00	00	01	10	11	00	00	01	10	11
		00	$\frac{1}{4}$	$\frac{1}{4}$	$\frac{1}{4}$	$\frac{1}{4}$	00	$\frac{1}{4}$	0	0	1
		01	$\frac{1}{4}$	$\frac{1}{4}$	$\frac{1}{4}$	$\frac{1}{4}$	01	0	$\frac{1}{4}$	1	0
		10	$\frac{1}{4}$	$\frac{1}{4}$	$\frac{1}{4}$	$\frac{1}{4}$	10	0	1	$\frac{1}{4}$	0
		11	$\frac{1}{4}$	$\frac{1}{4}$	$\frac{1}{4}$	$\frac{1}{4}$	11	1	0	0	$\frac{1}{4}$

Table 1: FDTs of 2-bit variables

**Statistical model:** By injecting a fault in an operation an intermediate value of  $n$ -bit is affected. The intermediate value is represented by the two random variables  $S$  and  $S'$ , before and after the injected fault. This means the intermediate value is denoted by the random variable  $S$  when no faults are present and  $S'$  otherwise. Both random variable can take values  $s \in \mathcal{S} = \{0, \dots, 2^n - 1\}$ . The probabilities of the individual entries of the FDT are calculated as shown in Eq. (1), where  $s$  corresponds to the values in the rows and  $s'$  to the values in the columns of Table 1.

$$p_s(s') := P(S' = s' \mid S = s). \quad (1)$$

The elements of the diagonal of an FDT correspond to the probabilities for different ineffective faults as shown in Eq. (2).

$$p_{s'}(s') := P(S' = s' \mid S = s'). \quad (2)$$

We assume the FDT is not known to the attacker. Nevertheless, it is still possible to exploit the diagonal's deviation from the uniform distribution. Since we assume the presence of a detection-based countermeasure, or an authenticated decryption like GIMLI-decrypt (which inherently provides the required filtering), we will state the statistical model explicitly for this scenario. Here, the attacker has only access to samples where the intermediate values under attack fulfill  $S = S'$ . Under the assumption, that  $S$  is uniformly distributed with  $P(S = s) = 2^{-n} = \frac{1}{|\mathcal{S}|}$ , the rate of ineffective faults  $r_{\text{ineff}}$  can be calculated as shown in Eq. (3).

$$r_{\text{ineff}} = P(S' = S) = \sum_{s' \in \mathcal{S}} \frac{p_{s'}(s')}{|\mathcal{S}|} \quad (3)$$

The diagonal of the FDT can be expressed as conditional distribution as shown in Eq. (4). This distribution is later estimated by an attacker, as neither the diagonal nor  $S'$  can be observed.

$$p_{\text{ineff}}(s') = P(S' = s' \mid S' = S) = \frac{p_{s'}(s')}{|\mathcal{S}| \cdot r_{\text{ineff}}} \quad (4)$$

However, it is possible to calculate the hypothetical distribution  $p_H$  of  $S'_H$  under the assumption of a fixed key hypothesis  $k_H$ . By using the correct key guess  $k_H$  the correct distribution  $p_{\text{ineff}}(s') = p_{H=\text{correct}}(s')$  is observed. In order to distinguish it from incorrect key guesses, we assume that all distributions of incorrect key hypotheses  $k_{H=\text{wrong}}$  are close to the uniform distribution i.e.  $p_{H=\text{wrong}}(s') \approx \theta(s') = 2^{-n}$ . The distinguisher  $D(p_H)$  is used to rank the key candidates according to their distance to  $\theta(s')$ . The chi-squared ( $\chi^2$ ) test as introduced by Pearson [10], is used to calculate a metric for the difference of two probability distribution function  $a$  and  $b$ , both with values  $x \in \mathcal{X}$  and  $N$  samples as shown in Eq. (5)

$$\chi^2(a, b) = N \sum_{x \in \mathcal{X}} \frac{a(x) - b(x)}{b(x)}. \quad (5)$$

Since incorrect key guesses follow the uniform distribution, we can use the  $\chi^2$  metric to distinguish distributions resulting from the correct key hypothesis  $p_{H=\text{correct}}$  and a uniform distribution  $\theta$  caused by an incorrect hypothesis. This leads to the  $\chi^2$ -distinguisher as shown in Eq. (6).

$$D(p_{H_i}) = \text{CHI}(p_{H_i}) := \chi^2(p_{H_i}, \theta) \quad (6)$$

Alternatively, a scaled version of CHI, the Squared Euclidean Imbalance (SEI) [12] as shown in Eq. (7), can be used.

$$D(p_{H_i}) = \text{SEI}(p_{H_i}) = \frac{1}{|\mathcal{S}| \cdot N} \cdot \text{CHI}(p_{H_i}) \quad (7)$$

Where  $N$  denotes the number of observed decryptions under the influence of ineffective faults.

#### IV. GIMLI

GIMLI is a suite of cryptographic primitives based on the GIMLI-permutation by Bernstein et al. [1]. It participates in the NIST lightweight cryptographic project for authenticated encryption and hash. In this paper, we focus on the GIMLI-CIPHER, a family for Authenticated Encryption with Associated Data (AEAD).

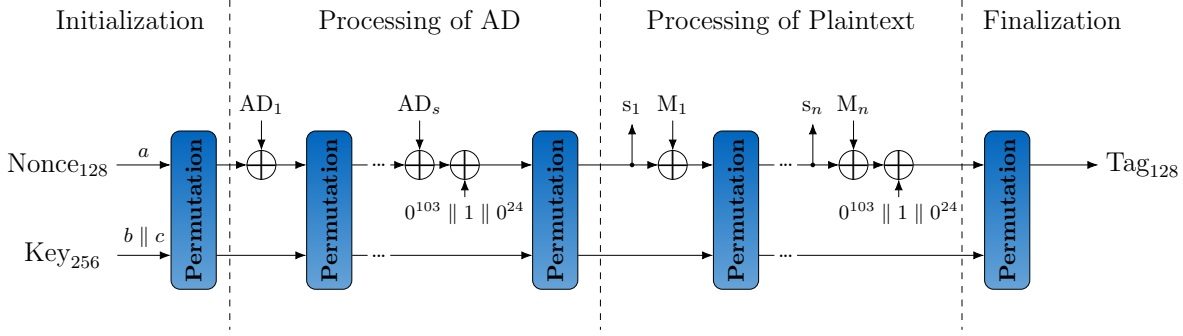


Figure 3: Sponge construction of GIMLI

#### A. The Gimli-permutation

The GIMLI-permutation is based on an 8x8-bit state. As shown in Eq. (8), the state is defined as a  $3 \times 4$  matrix: the rows are named  $a, b, c$ ; the columns are enumerated 0, 1, 2, 3; the round is denoted by  $r$ . For example  $a_1^{11}$  denotes to the second 32 bit word before the execution of the 11 round.

$$\text{State} := \begin{pmatrix} a_0^r & a_1^r & a_2^r & a_3^r \\ b_0^r & b_1^r & b_2^r & b_3^r \\ c_0^r & c_1^r & c_2^r & c_3^r \end{pmatrix} \quad (8)$$

Algorithm 1 describes how this state is permuted in 24 consecutive rounds. They are enumerated in reverse order: a permutation starts with round 24 and ends with round 1. During each round, the state is first substituted and permuted (SP-Box). Every second round, the state is mixed linearly (alternating either a small swap or a big swap). Finally, every fourth round, a constant is added.

#### Algorithm 1 The GIMLI-permutation

```

function PERMUTE( $a, b, c$ ) ▷ Input State
  for  $r = 24$  down to 1 do
    for  $j = 0$  to 3 do
       $t_a \leftarrow a_j \lll 24$  ▷ SP-Box
       $t_b \leftarrow b_j \lll 9$ 
       $t_c \leftarrow c_j$ 
    end for
    if  $r \bmod 4 = 0$  then
       $a_0 \parallel a_1 \parallel a_2 \parallel a_3 \leftarrow a_1 \parallel a_0 \parallel a_3 \parallel a_2$  ▷ Small Swap
    else if  $r \bmod 4 = 2$  then
       $a_0 \parallel a_1 \parallel a_2 \parallel a_3 \leftarrow a_2 \parallel a_3 \parallel a_0 \parallel a_1$  ▷ Big Swap
    end if
    if  $r \bmod 4 = 0$  then
       $a_0 \leftarrow a_0 \oplus 0x9e377900 \oplus r$  ▷ Constant Addition
    end if
  end for
  return  $(a, b, c)$  ▷ Output State
end function

```

#### B. The Gimli-AEAD

The GIMLI-CIPHER is a sponge based AEAD scheme with a 128 bit rate and a 256 bit capacity. The rate matches  $a$ , the capacity matches the concatenation of  $b$  and  $c$ . Fig. 3 depicts the four phase during an AEAD. As the exploited fault is ineffective in respect to the output, the exact behavior of the AEAD scheme is secondary and a brief description of the four phases is sufficient: First, the state is initialized with a 128 bit nonce, and the 256 bit key as depicted in Eq. (9).

$$\begin{aligned} \text{Nonce: } & a_0^{24} \dots a_3^{24} \leftarrow n_0 n_1 n_2 n_3 \\ \text{Key: } & b_0^{24} \dots b_3^{24} \parallel c_0^{24} \dots c_3^{24} \leftarrow k_0 k_1 \dots k_7 \end{aligned} \quad (9)$$

Second, the associated data  $AD_i$  are absorbed in blocks of 128 bit. Subsequently, the message block key  $s_i$  is squeezed. Depending on the mode, either the ciphertext  $C_i = M_i \oplus s_i$  or the plaintext  $M_i = C_i \oplus s_i$  is generated. In any case, next, the plaintext  $M_i$  is absorbed. Finally, the tag is calculated. Between all phases and absorbed blocks the GIMLI-permutation is invoked. Incomplete blocks are padded. Additionally, there is a domain separation between the processing of AD, the processing of plaintext, and finalization. For decryption, the tag is not output, but compared to the received tag. If both tags match, the plaintext is released, otherwise, the empty string is output.

#### V. SIFA ON GIMLI

We target the decryption of GIMLI because AEAD schemes only release the plaintext if the computed tag matches the original tag. This behavior can be exploited to distinguish between effective and ineffective faults, as an effective fault results in a tag mismatch.

##### A. Fault Injection Location

For the SIFA on GIMLI we evaluated different locations where an induced ineffective fault can be exploited. Similar to the attacks on Ketje and Keyak [5], we use the nonce and a hypothesis of the target partial subkey  $k_H$  to calculate an intermediate value of GIMLI. In general, this is possible

for any intermediate value during the decryption of GIMLI. However, in order to reduce the number of involved key-bits of the intermediate value and the number of hypotheses  $N_H$ , it is desirable to attack the early rounds of the first GIMLI-permutation. Fig. 4 shows an attack mounted during the initialization phase. When we target the first GIMLI-permutation, we can choose from one of the 24 rounds. The Substitution Permutation Box (SP-Box) of the GIMLI-permutation poses the best attack target, due to the involved non-linearity. A possible position to inject an ineffective fault into the SP-Box is colored **red** in Fig. 5. We mount the attack on a biased  $b^r$ , however a similar reasoning can be applied for a biased  $a^r$  or  $c^r$ . The attacked round is a trade-off between the number of recoverable key-bits  $n_{\text{keybits}}$  and number of possible key hypotheses  $N_H$ . The earlier the attack, the simpler are the equations for the intermediate values, but also fewer key bits can be revealed. The later the attack, the higher is the number of involved key bits  $n_{\text{keybits}}$  and thus, more hypotheses  $N_H$  must be checked. The number of hypotheses  $N_H$  grows exponentially with the number of involved key bits  $n_{\text{keybits}}$  as shown in Eq. (10).

$$N_H \sim 2^{n_{\text{keybits}}} \quad (10)$$

In order to determine the exact number of involved key bits  $b_k$  the dependencies of an intermediate value must be traced back to the initialization phase where the state gets initialized using the known nonce and the unknown key.

### B. Calculation of Intermediate Values

The dependencies of an intermediate value under attack are related to the fault injection location. We will demonstrate an attack of bit  $b_{0,7}^r$ . Hereby  $b_{0,7}^r$  denotes the seventh bit of the word  $b_0^{22}$  during round  $r$ . The resulting dependencies of  $b_{0,7}^r$  with respect to the according injection location are shown in the second row of Table 2. A fault injection in the very first

$r$	$n_{\text{keybits}}$	Dependencies of $b_{0,7}^r$
23	2	$k_{0,31} \oplus n_{0,15} \oplus (n_{0,14} \mid k_{4,6})$ $k_{0,21} \oplus n_{0,6} \oplus (n_{0,5} \mid k_{4,29}) \oplus k_{5,15} \oplus k_{1,6} \oplus$
22	11	$\oplus (n_{1,20} \& k_{1,3}) \oplus c_{15} \oplus [(k_{5,14} \oplus k_{1,5} \oplus (n_{1,19} \& k_{1,2}) \oplus c_{14}) \mid (n_{0,14} \oplus k_{4,5} \oplus (k_{4,4} \& k_{0,27}))]$
21	37	cf. Appendix

Table 2: Dependencies of  $b_{0,7}^r$  for different injection locations

round, i.e. after round 24, to attack the bit  $b_{0,7}^{23}$  only affects two key bits and therefore, does not offer a big advantage in terms of recoverable key bit this is shown in the first row of Table 2. If the fault is injected one round later i.e. after round 23, eleven key bits are involved in the computation of the bit  $b_{0,7}^{22}$  this is shown in the second row of Table 2. By biasing the intermediate bit  $b_{0,7}^{21}$  again a round later, an attacker can utilize 37 involved key-bits due to the sheer length of the involved equations we stated the full dependency equation in the Appendix. Involved key-bits lead to a dependency due to

the path along which they properagate through the GIMLI-permutation. The bit wise dependencies after each GIMLI-round are visualized similarly to Dobraunig et al. [4]. Involved bits i.e. dependencies are represented by a 1 independent bits are represented by '0' or '-' e.g.  $c=1100$  means that only bit 3 and 2 of this nibble are involved in a computation. The position of the key is colored in **green** and the nonce in **blue**. Fig. 6 shows, which bits are involved in the computation of the intermediate bit  $b_{0,7}^{22}$  which is colored in **red**. Even though 11 bits of the key are involved in the calculation of the intermediate value  $b_{0,7}^{22}$ , not all of them can be identified distinctively due to linear dependencies of the involved key bits. Eq. (11) shows these linear dependencies. Each of the three sums are affected by three different key bits. Therefore, only the sums  $k_{s1}$ ,  $k_{s2}$  and  $k_{s3}$ , but not the individual key bits can be recovered.

$$\begin{aligned} k_{s1} &= k_{0,21} \oplus k_{5,15} \oplus k_{1,6} \\ k_{s2} &= k_{5,14} \oplus k_{1,5} \\ k_{s3} &= k_{4,5} \oplus (k_{4,4} \& k_{0,27}) \end{aligned} \quad (11)$$

Thus, an attack on the intermediate value  $b_{0,7}^{22}$  reveals only the key bits  $k_{4,29}$ ,  $k_{1,3}$  and  $k_{1,2}$ . However, the key sums can also be used to build hypotheses. This results in an advantage of  $2^6$  compared to brute-forcing each individual bit of the involved key bits. An attack on the intermediate state  $b_{0,7}^{21}$  already involves 37 key bits. Taking linear dependencies into account, the number of hypotheses is  $2^{22}$ . A graphical representation of the dependencies of  $b_{0,7}^{21}$  is shown in Fig. 7 Going one round further ( $b_{0,7}^{r=20}$ ) increase the number of involved key bits to 168. However, testing  $2^{168}$  hypotheses is not feasible in a reasonable amount of time. Thus, the attack on the intermediate states in rounds 22 and 21 offer a reasonable trade-off between the number of hypotheses and recoverable key bits.

### C. Fault Model

In Section III the influence of some typical fault models onto the FDT's was shown in Table 1 at the example of a two bit intermediate state. However, the fault models are not limited to 2-bit but can be applied to words with variable width  $w$ . Since we cannot choose the word-width of the implementation of GIMLI but still want to evaluate the distribution of a single bit, it is important to evaluate, if a byte based fault model also biases each bit separately. For example a fault of width  $w = 8$  is the equivalent to a byte based fault model. We simulated faults with  $w = 8$  according to the probabilistic bit flip fault model where a flip from  $1 \rightarrow 0$  occurs with probability  $P_{1 \rightarrow 0} = \frac{2}{3}$  and a flip  $0 \rightarrow 1$  with probability  $P_{0 \rightarrow 1} = \frac{1}{3}$ . This biased bit flip probabilities for a one bit intermediate value  $b$  result in the histogram shown in Fig. 8 This behavior is the same as the FDT shown in Table 1d which depicts the two dimensional case. The bias of the 8-bit intermediate value  $b_{0,0-7}^{r=22}$  caused by an ineffective fault is shown in Fig. 9. The nearly normal distributed values without any fault are colored in **green** whereas all values leading to ineffective faults are colored in **blue**. If one compares the histogram as shown

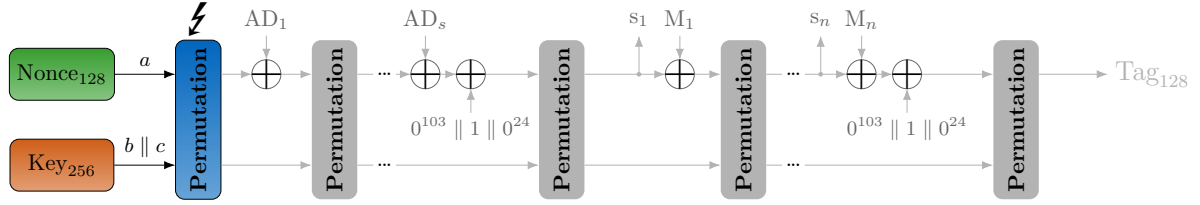


Figure 4: Fault Injection Location GIMLI

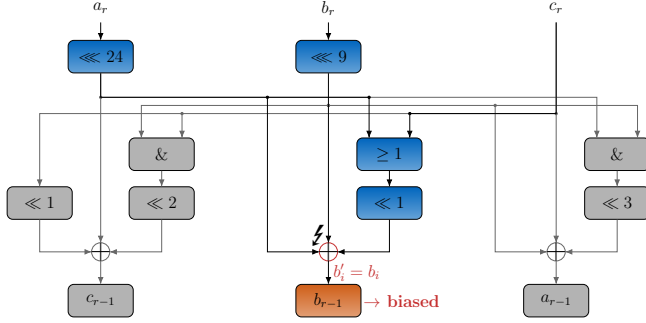


Figure 5: Fault Injection Location SP-Box

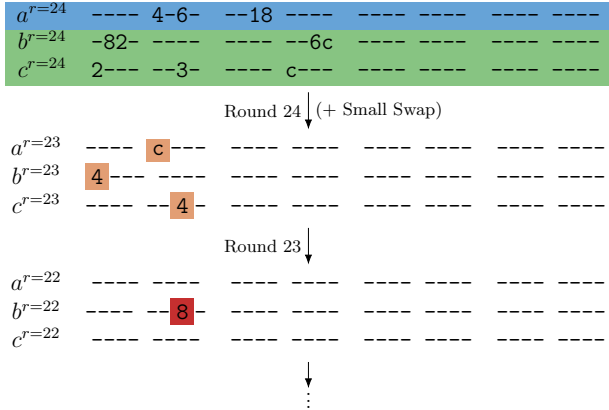


Figure 6: Dependencies of  $b_{0,7}^{r=22}$

in Fig. 9 with the previously introduced FDTs as shown in Table 1, it becomes clear that this distribution can be attacked due to the deviation from the uniform distribution which is directly recognizable. Based on the simulations as shown in Fig. 9 we decided to use a byte based fault model i.e.  $w = 8$  during the explanation of the attack strategy.

#### D. Attack Strategy

For the attack it is necessary to generate decryptions under the influence of an ineffective fault. As a result of GIMLI being a AEAD scheme the collected decryptions are all under the influence of an ineffective fault otherwise there would be

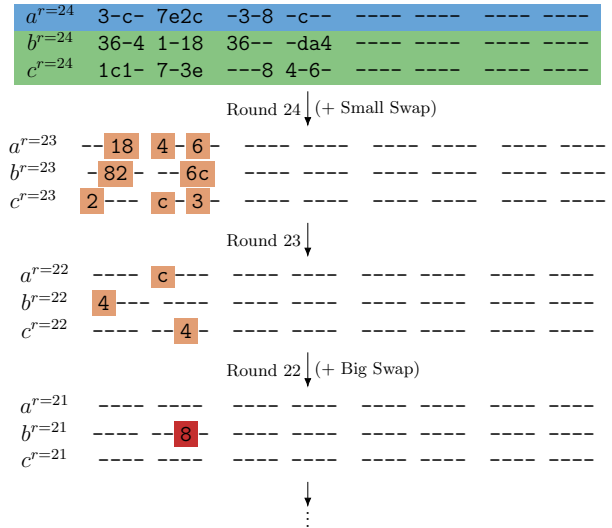


Figure 7: Dependencies of  $b_{0,7}^{r=21}$

no output due to a tag mismatch. After a sufficient number of decryptions  $N_d$  is obtained we calculate the hypothetical intermediate bit *inter*. The calculation of the intermediate bit is done with respect to the possible key hypotheses and all obtained nonces  $n$ . The distribution of *inter* is then ranked by according to the SEI. Now that each hypothetical distribution has been assigned an SEI, the correct key hypothesis can be identified as the one with the largest SEI. The algorithmic representation of the attack is shown in Algorithm 2. First the hypothetical intermediate values are calculated for all possible keys. Then for each key hypothesis the SEI of the intermediate distribution is calculated and stored. If a new SEI is greater than or equal to the old one the corresponding key hypothesis is used as the new correct hypothesis. After all hypotheses have been processed, the algorithm terminates. In our attack strategy, it is necessary to choose an appropriate intermediate value to attack as the involved key bits which can be recovered for each intermediate value differ. As introduced in Section V-B, it is possible to calculate some key bits directly and some key bits only in the form of a sum. The computation of the intermediate state  $b_{0,7}^{r=22}$  involves 11 key bits as shown in the dependency equations in Table 2. However, 8 key bits

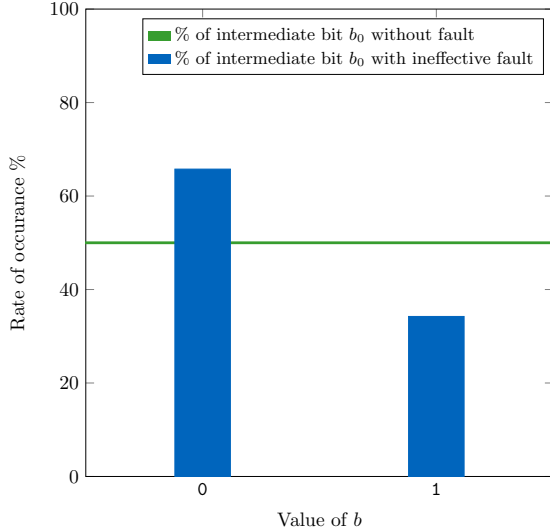


Figure 8: Histogram of intermediate values  $b$

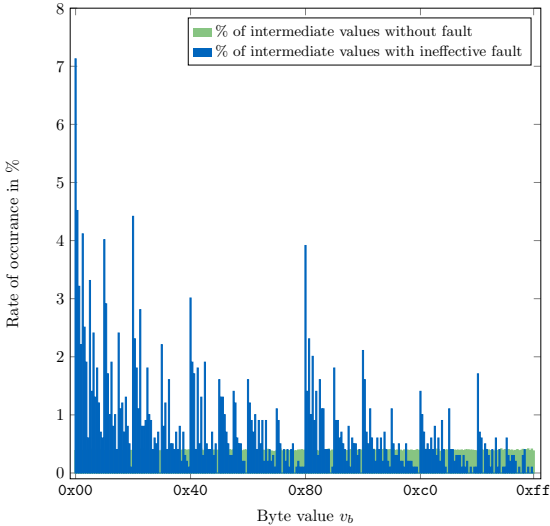


Figure 9: Histogram of intermediate values  $b_{0,7}^{r=22}$

influence  $b_{0,7}^{22}$  only in the form of a sum as shown in Eq. (11). The computation of  $b_{0,7}^{r=22}$  involves  $n_{\text{keybits}} = 11$  but only hypotheses on 6 key bits are required as the remaining key bits only appear in the form of a sum. Therefore, the number of hypotheses  $N_H$  shrinks from  $2^{11}$  to  $2^6$ . The same effect also occurs when we target the intermediate value at the same position one round later i.e.  $b_{0,7}^{r=21}$ . The computation of the intermediate state  $b_{0,7}^{21}$  involves 37 key bits as shown in the dependency equations in Table 2. The key-bits  $k_{4,26}$ ,  $k_{4,20}$ ,  $k_{4,5}$ ,  $k_{4,4}$ ,  $k_{4,3}$ ,  $k_{4,2}$ ,  $k_{4,1}$ ,  $k_{1,26}$ ,  $k_{1,25}$ ,  $k_{1,8}$ ,  $k_{1,7}$ ,  $k_{1,2}$ ,  $k_{0,26}$ ,  $k_{0,25}$  and  $k_{0,18}$  can be determined uniquely. Furthermore, the sum of 22 key bits in the form of 7 sum can be determined. From the 37 involved key bits we are able to obtain an advantage of 22 bits compared to the brute force effort over

---

## Algorithm 2 SIFA on GIMLI

---

```

 $N_H \leftarrow 2^{n_{\text{keybits}}}$ 
 $n[N_d] \leftarrow \text{loadNonces}()$ 
 $\text{maxSEI} \leftarrow 0$ 
 $\text{corrHypo} \leftarrow 0$ 
 $\text{for } i = 0 \text{ to } N_H \text{ do}$ 
 $\quad \text{for } j = 0 \text{ to } N_d \text{ do}$ 
 $\quad \quad \text{inter}[i][j] \leftarrow \text{calcIntermediateBit}(i, n[j])$ 
 $\quad \text{end for}$ 
 $\quad \text{SEI}[i] \leftarrow \text{calcSEI}(\text{inter}[i][*])$ 
 $\quad \text{if } \text{SEI}[i] \geq \text{maxSEI} \text{ then}$ 
 $\quad \quad \text{maxSEI} \leftarrow \text{SEI}[i]$ 
 $\quad \quad \text{corrHypo} \leftarrow i$ 
 $\quad \text{end if}$ 
 $\text{end for}$ 
 $\text{return corrHypo}$ 

```

---

all involved key bits. Due to some ambiguity in the large equation for  $b_{0,7}^{r=21}$  the SIFA reveals three candidates with the same SEI after 340 decryptions under the influence of ineffective faults. The ambiguity is caused by some nonce bits that do not differ when they cause an ineffective fault. Although the described ambiguity is present, there is always the correct key-hypothesis among those three candidates. By the injection of 8-bit ineffective fault, hypotheses can be build on 8 intermediate bits that can be evaluated simultaneously with almost no extra computational effort. With this we get an advantage of at most  $8 \cdot 6 = 48$  bits when attacking round 22 and at most  $8 \cdot 22 = 176$  bits when attacking round 21. In order to obtain the complete key which is loaded during the initialization phase of GIMLI it is necessary to repeat the proposed attacks with varying intermediate states under attack until all key bits are recovered.

## VI. RESULTS

Now that we have clarified the prerequisites for the attack, we will present the results. First we will evaluate the influence of the fault width  $w$  on the ineffectiveness rate of the injected faults. Second the obtained results for the attack on  $b_{0,7}^{r=22}$  and  $b_{0,7}^{r=21}$  are presented. Both attacks exploit the bias of an ineffective fault with fault width  $w = 8$  bit injected after round 23 respectively 22 under the assumption of a probabilistic bit flip fault model.

### A. Influence of fault width on ineffectiveness rate

SIFA exploits the bias present in an intermediate state independently of the assumed fault model. In practice, it is usually assumed that an attacker has no information about the FDT which is caused by the ineffective fault injection. Nevertheless, the only prerequisite for a successful attack is that an intermediate value follows a biased distribution. The biased distribution is indicated by the diagonal of the FDT which follows a non-uniform distribution as shown in Table 1. Furthermore, we typically cannot choose the target architecture where GIMLI-AEAD is run on, which can either be a software implementation running on a microcontroller or a hardware implementation running on a FPGA or ASIC. If we consider the case of a software implementation of GIMLI-AEAD, then the fault width  $w$  will be the same as the word width of the

micro-controller. If we consider a hardware implementation of GIMLI-AEAD the fault width  $w$  is usually dependent of the implementation. In the following we use the typical fault models random-And, Stuck-at-0 and probabilistic bit-flip exemplary to simulate a fault on a software implementation, the same reasoning can also be applied to hardware implementations. Faults are injected during round 23 of the first GIMLI-permutation on state  $b_0^{r=22}$ . The width  $w$  of the fault ranges from 1 to 32 bit with  $w \in \{1, 4, 8, 16, 32\}$ . By calculating the number of ineffective faults  $n_{\text{ineff}}$  divided by the number of total encryptions  $N$  we obtain the ineffectiveness rate as shown in Eq. (12).

$$r_{\text{ineff}} = \frac{n_{\text{ineff}}}{N}. \quad (12)$$

The ineffectiveness rate  $r_{\text{ineff}}$  with respect to the fault width  $w$  is shown in Fig. 10. As one can see the ineffectiveness

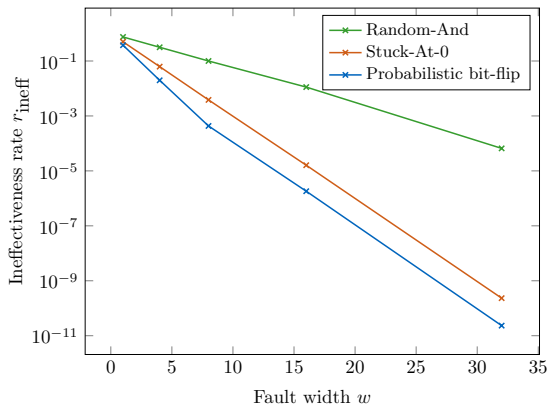


Figure 10: Ineffectiveness rate  $r_{\text{ineff}}$  of different fault models

rate  $r_{\text{ineff}}$  decreases almost linearly with the assumed fault width  $w$ . The linear decrease of the ineffectiveness rate occurs independently of the three fault models. The ineffectiveness rate of the probabilistic bit flip fault model is dependent on the assumed bit flip probabilities we decided to use this model to provide a worst case estimation. In practice this means that attacking a 32-bit software implementation of GIMLI, should be feasible according to Fig. 10. Especially the Random-And model offers a significant rate of ineffective faults at  $w = 32$  bit. However, due to the very low ineffectiveness rate for the other fault models, a number of more than  $10^9$  total encryptions is required for the attack. For the sake of simplicity further simulations were done with a fault width  $w = 8$  bit in order to minimize the computational effort of generating ineffective faults.

#### B. Attack on $b_{0,7}^{r=22}$

The attack on the intermediate state  $b_{0,7}^{r=22}$  is able to retrieve the involved key bits correctly after approximately 180 ineffective faults. The number of required encryptions under the influence of an ineffective fault is shown in Fig. 12 where we used the SEI as statistical metric. In Fig. 12 the best wrong hypothesis is colored red and the correct hypothesis

in blue. Furthermore, it is important to notice, that after the point both are crossing line, the correct hypothesis keeps a significantly higher value. Fig. 11 shows the advantage over brute forcing when increasing the number of decryptions with ineffective faults. The maximum advantage is defined as the number of unique definable parameters when attacking the single bit  $b_{0,7}^{r=22}$ , i.e. the three key-bits and the three sum-values therefore the maximal advantage of the attack on round 21 can be 6 bit. The unstable advantage at the beginning is caused by multiple key hypotheses with similar SEI values, which leads to frequent change of the key hypothesis having the current maximum SEI. Although the correct key hypothesis is retrieved after 180 ineffective faults, some bits of a wrong hypothesis still are equal to the corresponding bits in the correct guess leading to an advantage of less than 6 bits.

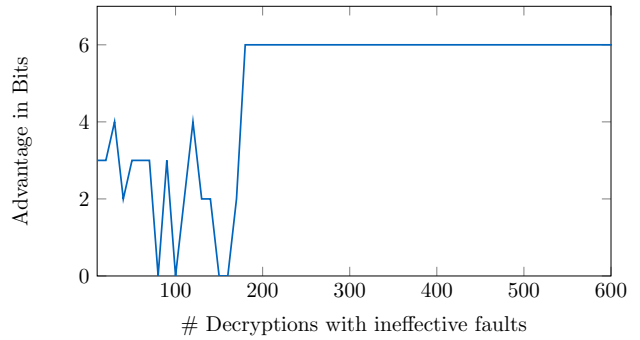


Figure 11: Advantage - Attack on round 22

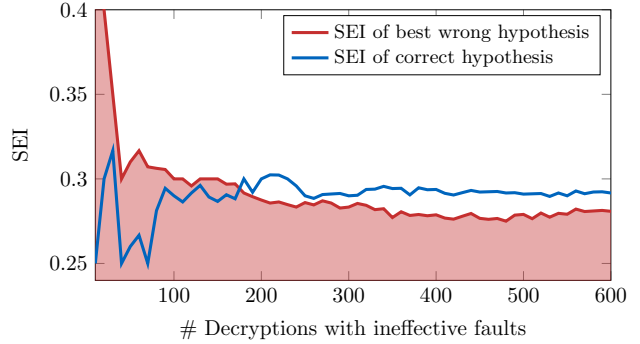


Figure 12: SEI - Hypotheses, round 22

#### C. Attack on $b_{0,7}^{r=21}$

The attack on the intermediate state  $b_{0,7}^{r=21}$  is able to retrieve the involved key bits correctly after approximately 340 ineffective faults. Again, the number of required encryptions under the influence of an ineffective fault is shown in Fig. 14 where we used the SEI as statistical metric. In Fig. 14 the best wrong hypothesis is colored red and the correct hypothesis is blue. Fig. 13 shows the advantage over brute forcing when increasing the number of decryptions with ineffective faults.

The possible advantage when attacking  $b_{0,7}^{r=21}$  is 22-bits at max. Although the hypothesis with highest SEI changes frequently when using less than 340 ineffective faults, the correct key-guess has the maximal SEI after obtaining it.

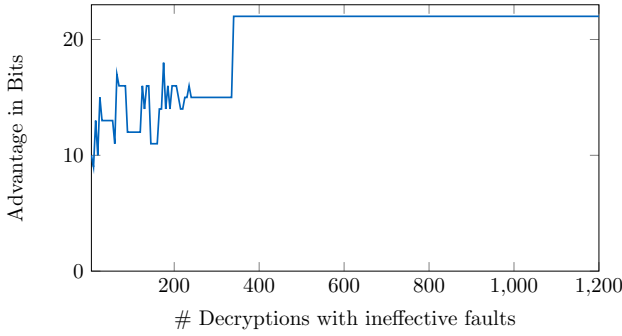


Figure 13: Advantage - Attack on round 21

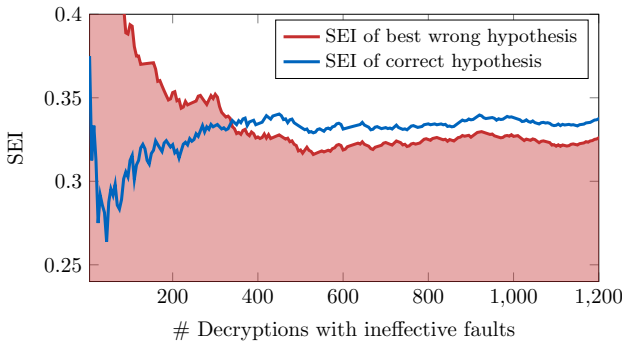


Figure 14: SEI - Hypotheses, round 21

## VII. CONCLUSION

In this work we presented the SIFA of the AEAD scheme GIMLI (GIMLI-24-CIPHER). Furthermore, we investigated the influence of the fault width  $w$  on the rate of ineffective faults  $r_{\text{ineff}}$ . The fact that SIFA can be applied to the AEAD scheme GIMLI should be considered a threat. This is mainly due to the fact that the fault model assumed by SIFA is rather simple to achieve i.e. a biased intermediate value which is processed during a cryptographic operation. Due to the ineffective characteristic common countermeasures against fault attacks can be circumvented by SIFA.

## ACKNOWLEDGEMENTS

We would like to thank the anonymous reviewers for their valuable comments and suggestions on the paper, as these helped us to improve it. This work was partly funded by the German Federal Ministry of Education and Research in the project HQS through grant number 16KIS0616.

## REFERENCES

- [1] Daniel J Bernstein et al. “Gimli: a cross-platform permutation”. In: *International Conference on Cryptographic Hardware and Embedded Systems*. Springer. 2017, pp. 299–320.
- [2] Dan Boneh, Richard A. DeMillo, and Richard J. Lipton. “On the Importance of Eliminating Errors in Cryptographic Computations”. In: *Journal of Cryptology* 14.2 (2000), pp. 101–119. DOI: 10.1007/s001450010016.
- [3] Christophe Clavier. “Secret external encodings do not prevent transient fault analysis”. In: *International Workshop on Cryptographic Hardware and Embedded Systems*. Springer. 2007, pp. 181–194.
- [4] Christoph Dobraunig, Maria Eichlseder, and Florian Mendel. *Heuristic Tool for Linear Cryptanalysis with Applications to CAESAR Candidates*. Cryptology ePrint Archive, Report 2015/1200. <https://eprint.iacr.org/2015/1200>. 2015.
- [5] Christoph Dobraunig et al. *Fault Attacks on Nonce-based Authenticated Encryption: Application to Keyak and Ketje*. Cryptology ePrint Archive, Report 2018/852. <https://eprint.iacr.org/2018/852>. 2018.
- [6] Christoph Dobraunig et al. “SIFA: exploiting ineffective fault inductions on symmetric cryptography”. In: *IACR Transactions on Cryptographic Hardware and Embedded Systems* (2018), pp. 547–572.
- [7] Thomas Fuhr et al. “Fault attacks on AES with faulty ciphertexts only”. In: *2013 Workshop on Fault Diagnosis and Tolerance in Cryptography*. IEEE. 2013, pp. 108–118.
- [8] Kerry McKay et al. *Report on lightweight cryptography*. Tech. rep. National Institute of Standards and Technology, 2016.
- [9] Sikhar Patranabis, Abhishek Chakraborty, and Debdeep Mukhopadhyay. “Fault Tolerant Infective Countermeasure for AES”. In: *Security, Privacy, and Applied Cryptography Engineering*. Springer International Publishing, 2015, pp. 190–209. DOI: 10.1007/978-3-319-24126-5\_12.
- [10] Karl Pearson. “X. On the criterion that a given system of deviations from the probable in the case of a correlated system of variables is such that it can be reasonably supposed to have arisen from random sampling”. In: *The London, Edinburgh, and Dublin Philosophical Magazine and Journal of Science* 50.302 (1900), pp. 157–175. DOI: 10.1080/14786440009463897.
- [11] Keyvan Ramezanpour, Paul Ampadu, and William Diehl. “A Statistical Fault Analysis Methodology for the Ascon Authenticated Cipher”. In: *2019 IEEE International Symposium on Hardware Oriented Security and Trust (HOST)*. IEEE, 2019. DOI: 10.1109/hst.2019.8741029.
- [12] Matthieu Rivain. “Differential Fault Analysis on DES Middle Rounds”. In: *Lecture Notes in Computer Sci-*

ence. Springer Berlin Heidelberg, 2009, pp. 457–469.  
 DOI: 10.1007/978-3-642-04138-9\_32.

[13] Jinbao Zhang et al. “Against fault attacks based on random infection mechanism”. In: *IEICE Electronics Express* 13.21 (2016), pp. 20160872–20160872.

## APPENDIX

### A. Dependency $b_{0,7}^{r=21}$ - round 22

$$b_{0,7}^{r=21} = b_{0,30}^{r=22} \oplus a_{0,15}^{r=22} \oplus (a_{0,14}^{r=22} \mid c_{0,6}^{r=22}).$$

### B. Dependency $b_{0,7}^{r=21}$ - round 23

$$\begin{aligned} b_{0,30}^{r=22} &= b_{0,21}^{r=23} \oplus a_{0,15}^{r=23} \oplus (a_{0,5}^{r=23} \mid c_{0,29}^{r=23}) \\ a_{0,15}^{r=22} &= c_{0,15}^{r=23} \oplus b_{0,6}^{r=23} \oplus (a_{0,20}^{r=23} \& b_{0,3}^{r=23}) \\ a_{0,14}^{r=22} &= c_{0,14}^{r=23} \oplus b_{0,5}^{r=23} \oplus (a_{0,19}^{r=23} \& b_{0,2}^{r=23}) \\ c_{0,6}^{r=22} &= a_{0,14}^{r=23} \oplus c_{0,5}^{r=23} \oplus (c_{0,4}^{r=23} \& b_{0,27}^{r=23}) \end{aligned}$$

### C. Dependency $b_{0,7}^{r=21}$ - input

$$\begin{aligned} b_{0,21}^{r=23} &= \mathbf{k_{0,12}} \oplus n_{0,29} \oplus (n_{0,28} \mid k_{4,20}) \\ a_{0,6}^{r=23} &= \mathbf{k_{5,6}} \oplus \mathbf{k_{1,29}} \oplus (n_{1,11} \& k_{1,26}) \oplus c_6 \\ a_{0,5}^{r=23} &= \mathbf{k_{5,5}} \oplus \mathbf{k_{1,28}} \oplus (n_{1,10} \& k_{1,25}) \oplus c_5 \\ c_{0,29}^{r=23} &= n_{0,5} \oplus \mathbf{k_{4,28}} \oplus (\mathbf{k_{4,27}} \& \mathbf{k_{0,18}}) \end{aligned}$$

$$\begin{aligned} c_{0,15}^{r=23} &= n_{0,23} \oplus \mathbf{k_{4,14}} \oplus (\mathbf{k_{4,13}} \& \mathbf{k_{0,4}}) \\ b_{0,06}^{r=23} &= \mathbf{k_{0,29}} \oplus n_{0,14} \oplus (n_{0,13} \mid k_{4,5}) \\ a_{0,20}^{r=23} &= \mathbf{k_{5,20}} \oplus \mathbf{k_{1,11}} \oplus (n_{1,25} \& k_{1,8}) \oplus c_{20} \\ b_{0,03}^{r=23} &= k_{0,26} \oplus n_{0,11} \oplus (n_{0,10} \mid k_{4,2}) \end{aligned}$$

$$\begin{aligned} c_{0,14}^{r=23} &= n_{0,22} \oplus \mathbf{k_{4,13}} \oplus (\mathbf{k_{4,12}} \& \mathbf{k_{0,3}}) \\ b_{0,05}^{r=23} &= \mathbf{k_{0,28}} \oplus n_{0,13} \oplus (n_{0,12} \mid k_{4,4}) \\ a_{0,19}^{r=23} &= \mathbf{k_{5,19}} \oplus \mathbf{k_{1,10}} \oplus (n_{1,24} \& k_{1,7}) \oplus c_{19} \\ b_{0,2}^{r=23} &= k_{0,25} \oplus n_{0,10} \oplus (n_{0,9} \mid k_{4,1}) \end{aligned}$$

$$\begin{aligned} a_{0,14}^{r=23} &= \mathbf{k_{5,14}} \oplus \mathbf{k_{1,5}} \oplus (n_{1,19} \& k_{1,2}) \oplus c_{14}; \\ c_{0,05}^{r=23} &= n_{0,13} \oplus k_{4,4} \oplus (k_{4,3} \& k_{0,26}) \\ c_{0,04}^{r=23} &= n_{0,12} \oplus k_{4,3} \oplus (k_{4,2} \& k_{0,25}) \\ b_{0,27}^{r=23} &= k_{0,18} \oplus n_{0,3} \oplus (n_{0,2} \mid k_{4,26}) \end{aligned}$$

### D. $b_{0,7}^{r=21}$ - key sums

Key bits which can only recovered in the form of a sum are colored in **blue**.